Experimental study of the performance of a heat exchanger for a new desalination-cooling technique using ice slurry: A proof of concept

Maria Aurely Yedmel, Ahmad Nasser Eddine, Hong-Minh Hoang, Romuald Hunlede, Laurence Fournaison, Anthony Delahaye

Applied Thermal Engineering 250 (2024) 123479

Contents lists available at ScienceDirect

Applied Thermal Engineering

journal homepage: www.elsevier.com/locate/apthermeng

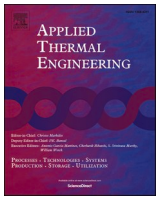

Research Paper

Experimental study of the performance of a heat exchanger for a new desalination-cooling technique using ice slurry: A proof of concept

Maria Aurely Yedmel [a,*], Ahmad Nasser eddine [a], Hong-Minh Hoang [a], Romuald Hunlede [a], Laurence Fournaison [a], Anthony Delahaye [a]

[a] Université Paris-Saclay, INRAE, FRISE, 92761 Antony, France

ARTICLE INFO

Keywords:
Desalination
Ice slurry
Melting
Finned-tube heat exchanger
Water
Cooling

ABSTRACT

Ice slurry was used to produce desalinated water and cold energy simultaneously. The process involved partially freezing seawater to separate the ice from the brine. Then, freshwater is produced by recovering heat from seawater to melt the ice. This paper focused on the kinetics and efficiency of ice melting in direct contact with a finned-tube heat exchanger. The melting performances were analysed as a function of the quantity of ice, the salt water flow rate and the state of the ice during melting. It was found that increasing the salt water flow rate by 33 % increased the melting efficiency by 33 % and decreased the melting time by 15 %. Increasing the quantity of ice by 36 % decreased the melting efficiency by 6 % and increased the melting time by 24 %. The use of weights impacted melting efficiency differently depending on the state of the ice (compacted, watered).

1. Introduction

As a result of the expansion of industrial activities and population growth, several countries have been facing a scarcity of natural freshwater [11]. Consequently, industrial processes have been developed for generating freshwater from brackish water. In their study, Curto et al. [5] categorised desalination processes into three main groups: evaporation and condensation techniques, filtration techniques, and crystallisation techniques.

The most energy-intensive processes in desalination are evaporation and condensation techniques, with Multi-Stage Flash units (MSF), Multi-Effect Distillation units (MED), and Mechanical Vapour Compression units (MVC) being the most commonly used methods [5]. To decrease the energy consumption of evaporation/condensation techniques, Darwish [6] proposed using MED units only, as they offer superior thermodynamic efficiency compared to MSF units. However, Sharon and Reddy [22] suggested coupling MED units with MSF units to achieve better overall efficiency.

Filtration desalination techniques involve the use of membranes to eliminate minerals and dissolved solids from water. Reverse Osmosis (RO) is the most adopted in this regard, as it produces high-purity water. This process typically involves four main steps, including water pre and post treatments, as well as the use of high-pressure pumps, which result in a significant energy consumption [5].

Freshwater production through crystallisation techniques involves a series of steps. It begins with seawater cooling, then ice crystallisation (fully or partially), ice separation from the brine and finally ice melting. Ongoing research is focusing on hydration and freezing methods. Desalination by hydration involves the formation of gas hydrates, which are crystalline solids composed of water molecules and gases such as nitrogen, carbon dioxide and methane [24]. According to [21], desalination of highly saline water (water with a salt content of 2.5 % − 6 %) requires less energy by hydration (clathrate method) than by MSF and RO techniques. The slow implementation of this technique is due to the high upfront investment costs.

Desalination by freezing can be classified into two categories: direct and indirect contact freezing. In direct contact freezing, a refrigerant is used in direct contact with the solution to be frozen. This method offers an efficient design, a high production rate, and a low driving force. However, in this method, the refrigerant must be water-immiscible, non-toxic, non-flammable, chemically stable, inexpensive, and commercially available [5]. Indirect contact freezing can be divided into two subtypes: cold plate and suspension freezing [3]. In this case, the refrigerant is used without direct contact with the solution. The advantage of cold surface crystallisation is that ice crystal formation occurs in a one-dimensional direction, causing layer-by-layer crystallisation. In this way, impurities are less trapped between the ice crystals. Ice slurries (suspension freezing) consist of a liquid blend containing water and an additional substance like alcohol, salt, or ammonia, with pure ice

* Corresponding author.
E-mail address: maria-aurely.yedmel@inrae.fr (M.A. Yedmel).

https://doi.org/10.1016/j.applthermaleng.2024.123479
Received 14 February 2024; Received in revised form 6 May 2024; Accepted 23 May 2024
Available online 24 May 2024

Nomenclature

ΔT	Temperature difference between inlet and outlet of the heat exchanger, °C
ε	Thickness,m
A	Heat transfer area,m^2
c_p	Specific heat capacity,J/(kg.°C)
D	Melting kinetic per unit area,kg/s.m^2
E	Melting efficiency, %
h	Height,m
l	Length,m
L	Specific latent heat,J/kg
LMTD	Logarithmic mean temperature difference, °C
m	Mass,kg
$\dot{m}$	Mass flow rate,kg/s
N	Number (quantity),/
$\dot{Q}$	Exchanged power,W
T	Temperature, °C
t	Time,s
U	Overall heat transfer coefficient,W/(m^2.°C)

Subscripts

fin	Heat exchanger fins
HE	Heat exchanger
i1	Heat exchanger inlet
i2	Air inlet
int	Internal
melt	Melting
min	Minimum
o1	Heat exchanger outlet
o2	Air outlet
st_wr	Salt water solution
MPET	Heat exchanger micro-multiport extrusion tubes
wr	Water

Abbreviations

C	Compacting
NC	No Compacting
NWg	No Watering
NWs	No Weights
PSU	Practical Salinity Unit
TC	Test Condition
Wg	Watering
Ws	Weights

crystals constituting 5–30 % of the mixture. The advantage of suspension freezing is the production of many small pure ice particles in the salt solution. If well removed, these ice crystals produce pure freshwater [3,25,19]. Suspension freezing has a low risk of scaling and corrosion with simple maintenance. Hybrid processes that combine crystallisation processes with other desalination methods are possible and being investigated [10]. Ice slurry is a well-known process for desalination but has rarely been linked to an energy recovery application. No studies have been conducted on ice melting in direct contact with a heat exchanger, particularly on ice from dry slurry. No research has combined direct contact ice melting with an energy recovery system. Instead, many researchers have focused on controlling the melting of ice crystals within the ice slurry in vertical/horizontal rectangular channels or tubes, heat exchangers and storage tanks to understand and improve heat transfer within the suspension [23,18,7,14,16].

An innovative desalination technique combining ice slurry with an energy recovery system is proposed in this paper (patent n°FR3114642). This novel process aims to produce freshwater and generate cold energy from seawater for various applications such as air conditioning and food preservation. The process involves several steps. The first step is partial freezing of the seawater. The second step consists of separating the ice crystals from the brine. The third step focuses on melting the ice crystals while recovering the cold energy for cooling purposes. Besides the high investment costs, the main challenges encountered in suspension freezing are the removal of the ice generated during the process and the chosen ice-melting technology. To overcome the difficulties of ice separation with ice slurries, Sharon and Reddy [22] proposed a practical way to remove the ice using two chambers, solenoid valves and a reversible heat pump. Lin et al. [12] suggested a system utilising the low temperatures available for the regasification of liquefied natural gas to produce freshwater from seawater. With their process, Lin et al. [12] obtained a salt removal rate of 50 %. For the novel desalination process presented in this paper, the separation stage was carried out using a laboratory spinner. Spinners are widely used in industry and laboratories to separate solids from liquids. Significant water salinity results were obtained using this method. In fact, the water salinity was reduced by a factor of 10. Once the ice has been separated from the brine, the next step is to recover the energy it contains. The best way to retrieve a large amount of cold energy (latent and sensible) and produce water simultaneously is to melt the ice completely. Therefore, it is necessary to determine the best type of heat exchanger to use for maximum efficiency. This stage is crucial because it will determine how well the entire desalination system is optimised. The objective is to maximise the recovery of cold energy from the ice and minimise the complexity of the melting stage.

Specific heat exchangers for ice melting are not well-defined. Existing heat exchangers are more or less suitable depending on the type of melting (dynamic or static), the heat exchanger's efficiency, and its compatibility with continuous processes. Dynamic melting aims to emphasise forced convection as forced convection exhibits a higher heat transfer coefficient compared to natural convection and conduction, which predominate in static melting. For dynamic melting, the screw heat exchanger is a viable option. The rotation of the screw facilitates the transportation of ice from the inlet to the outlet of the heat exchanger. Alternatively, the shell-and-tube heat exchanger has already been used for dynamic melting, with the liquefied ice being continuously recirculated using a pump [8]. Static melting presents some challenges, primarily due to the phase change at the heat exchanger surface. During the melting process, the solid/liquid boundary of the ice moves away from the heat transfer surface, leading to increased thermal resistance. However, if there is a thin liquid layer between the solid phase and the surface of the heat exchanger, the heat flux at the interface is significantly higher promoting faster phase change [9]. To further improve the heat transfer, finned-tube heat exchangers (circular, longitudinal, rectangular) are used. The quantity and dimensions of the fins play a significant role in reducing the melting time by increasing the effective heat transfer surface area [2]. When assembling fins and tubes, the quality and type of welded joints can also influence the mechanical and thermal properties of the material in these areas [1]. With this enormous heat transfer potential, finned tube heat exchangers are mainly studied for latent or sensible heat thermal storage (cold/hot water, pure ice, ice slurry and other phase change materials) [2,15,13,17,26]. For the cogeneration project, the heat exchanger to be used must be one in which the water from ice melting can flow unobstructed. The finned-tube heat exchanger seems to meet this requirement. However, no studies have been conducted on ice melting on top of a finned-tube heat exchanger.

This study aims to characterise the ice melting process on a finned-

tube heat exchanger by examining the melting kinetics and melting efficiency. The melting step is optimised according to various parameters: the quantity of ice, the flow rate of salt water, the state of the ice (compact or not), and the utilisation of weights or water. The purpose is to determine the most effective combination of these operating parameters to obtain efficient ice melting and to demonstrate, as a proof of concept, that ice melting on a finned tube heat exchanger is possible and certainly more practical for cogeneration systems.

2. Materials and methods

2.1. Process overview

The proposed seawater desalination process combines the production of freshwater with the generation of cold energy. Fig. 1 provides an overview of the process flow diagram for the desalination process. Initially, seawater undergoes pre-cooling in a primary heat exchanger, which serves to lower its temperature before entering a scraped-surface ice-slurry generator. This step is essential as it directly affects the cooling demand of the ice slurry generator. The generator blades continuously remove the ice formed on the surface of the heat exchanger, creating a slurry of ice particles. The slurry is then directed to a separator that separates the solid phase (ice) from the liquid phase (concentrated salt water). To enhance the energy efficiency of the process, the separated ice is sent back to the primary heat exchanger, where it is melted by the seawater. This step not only produces freshwater but also reduces the seawater's temperature without adding an external stream. A network of secondary heat exchangers is implemented to recover available cold energy from both the freshwater and the concentrated salt water. This recovered cold energy can be used, for example, to meet the cooling requirements of a hotel. The concentrated salt water is then discharged back into the sea at its original temperature, and the freshwater can be delivered to the hotel for various uses.

This article focuses solely on melting the recovered ice (snow) on the primary heat exchanger. A laboratory-scale experimental configuration was developed to investigate the kinetics and efficiency of ice melting. The experimental configuration includes three main components: the ice slurry generator, the spinner to separate ice crystals from the liquid, and the primary heat exchanger to melt the ice. Initially, a salt solution is cooled within the ice generator, resulting in the formation of the ice slurry. Afterwards, the spinner is employed to separate the ice crystals from the concentrated salt solution. Finally, the ice is subjected to the melting process, serving the dual purpose of pre-cooling the salt solution and generating freshwater. The experiments were carried out in batch processing (Fig. 2).

2.2. Experimental setup

2.2.1. Salt solution

To replicate the properties of seawater, the salt solution was prepared by mixing approximately 173 g of coarse sea salt (NaCl) with 5800 g of water. This composition aimed to achieve a salinity level of 30 PSU, which closely approaches the average seawater salinity, ranging from 33 PSU to 37 PSU [4]. All salinity measurements were carried out using a salinometer from Mettler-TOLEDO. Weighing was performed using a Sartorius CPA34001P balance.

2.2.2. Ice slurry production and ice separation

An ice slurry with 12 % of ice content was generated using a scraped surface heat exchanger (VALMAR "EASY TTi"). This equipment facilitated the continuous removal of ice formed on its walls, producing fine ice crystals. The generated ice slurry was then fed into a spinner (THOMAS, CENTRI 776 SEK, 2800 rpm) to separate the ice crystals from the saline phase, yielding a snow-like texture (Fig. 3).

2.2.3. Ice melting process

The ice melting process was carried out inside a cold chamber, set at 2 °C, to minimise ice melting caused by the ambient air. The main components of the system were a salt water tank, a thermostatic bath (JULABO, ED), an ultrasonic flowmeter (Bronkhorst, ES-FLOW-meter-with-pump) and a finned-tube heat exchanger (Fig. 2). A preliminary study to optimise the heat exchanger for ice melting has yet to be carried out. To prove the feasibility of the concept, a commercially available aluminium finned tube heat exchanger (TIIYEE, 12 micro-multiport extrusion tubes (MPET)) was used for the experiments. Fig. 4 illustrates the characteristics of the heat exchanger used.

First, the salt water is pumped from a tank located outside the cold room. It then passes through a thermostatic bath to achieve a specific and constant temperature of 23 °C (average maximum temperature of south France seas). However, due to the cooling effect in the cold room, the temperature of the salt water slightly decreases before entering the heat exchanger, despite the insulation of the pipes. Two calibrated T-type thermocouples with an uncertainty of 0.02 °C (k = 2) are placed at the inlet and outlet of the heat exchanger to measure the temperature of the salt water. The thermocouples were calibrated using a standard temperature probe and a thermostatic bath. These thermocouples are connected to a data acquisition system, enabling the recording and observation of temperature variations throughout the experiment. Finally, to complete the system, the chilled salt water exiting the heat exchanger is reintroduced into the salt water tank. An acrylic column was positioned on top of the heat exchanger to serve as a container for holding the ice. This material was chosen for its insulating and

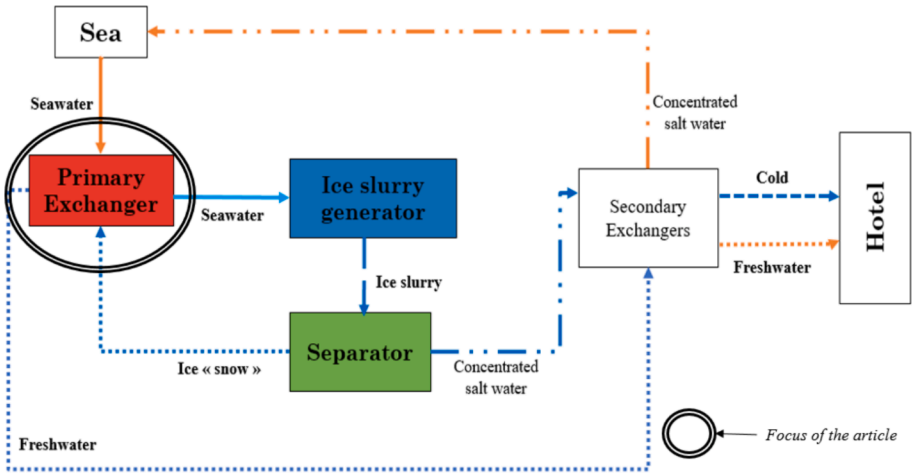

Fig. 1. Flow diagram of the desalination process.

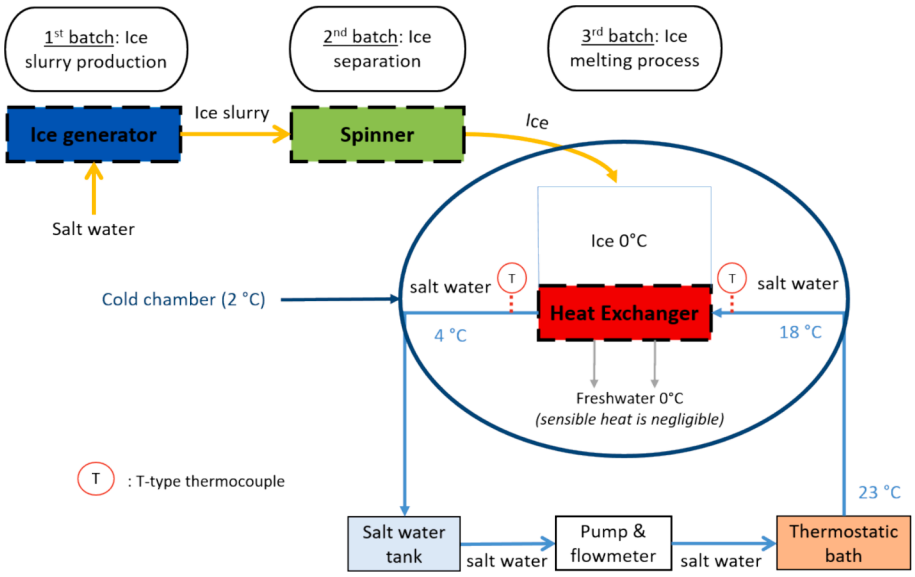

Fig. 2. Experimental set-up diagram with focus on ice melting process.

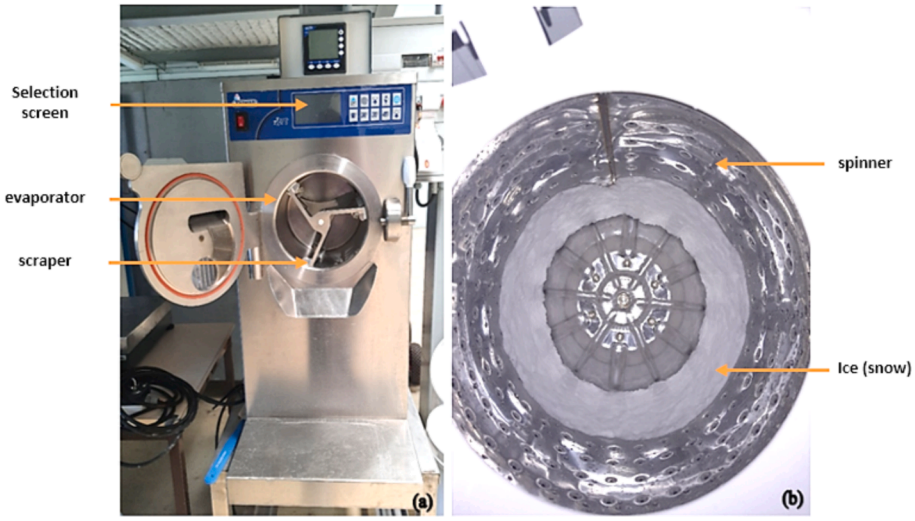

Fig. 3. Ice generator **(a)** and spinner **(b)** used for ice production.

transparent properties, enabling the state of the ice to be observed during the melting process. A custom-made 3D support is used to raise the heat exchanger, preventing direct contact with the melted ice tank. (Fig. 5).

2.3. Experimental protocol

The experimental procedure begins by preparing the salt water solution and activating the air conditioning system in the cold room. The data acquisition system for temperature measurement is also started. Once the outlet temperature of the heat exchanger has stabilised, the ice slurry production is initiated using the "Granita Silica" setting on the ice generator. When the crystals start to form, a 2-minute timer is started to achieve the desired ice fraction. The viscosity of the slurry is determined by the percentage of ice in the mixture. The more ice crystals form, the more viscous the slurry becomes. The ice slurry viscosity should be as low as possible for transport purposes inside process pipes. Here, 2 min corresponds to around 12 % of ice in the slurry. This percentage was calculated by dividing the total amount of ice collected from the spinner at the end of the separation stage by the mass of ice slurry recovered from the ice generator. When the timer reaches 2 min, the ice generator is stopped, and the slurry is transferred to the spinner to collect the ice crystals.

The collected ice is subjected to the melting experiments under various operating conditions. These conditions include the flow rate of salted water, the quantity of ice to be melted, the use of weights to force contact between the ice and the heat exchanger during melting at all times, the watering of the ice during melting and the compacting of the ice before melting (using a custom 3D hand-held tamper). Table 1 lists the experiments carried out for the ice melting process, and Fig. 6 provides a visual example of each type of experiment.

To ensure repeatability in the experiments where the ice was compacted, the ice height of the first experiment was noted and maintained for all following tests with the same quantity of ice (approximately 5 cm for 350 g and about 6 cm for 400 g).

In the case of watering experiments, a custom-made 3D water reservoir was used and filled with 2 mm in diameter glass marbles. Four holes of 2 mm diameter were drilled in the reservoir to facilitate further wetting of the coldest areas of the heat exchanger. In fact, during the experiment, without watering, a side of the heat exchanger (the side of

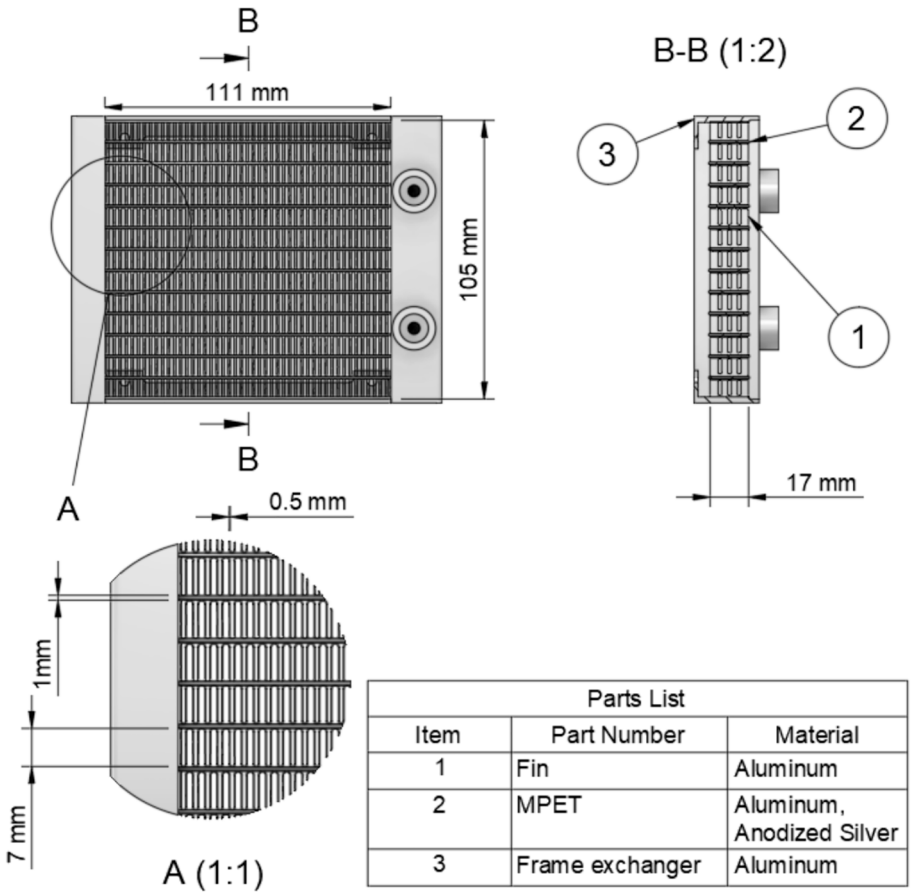

Parts List		
Item	Part Number	Material
1	Fin	Aluminum
2	MPET	Aluminum, Anodized Silver
3	Frame exchanger	Aluminum

Fig. 4. Detailed design of the finned tube heat exchanger.

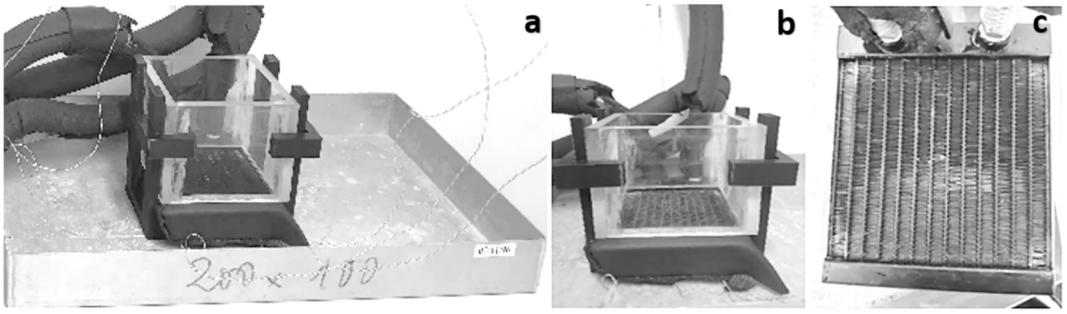

Fig. 5. Heat exchanger setup **(a)**: finned tube heat exchanger with **(b)** and without **(c)** acrylic column.

Table 1
Experiments carried out for ice melting process.

Test conditions	Number of experiments	Quantity of ice	Salt water flow rate	Compacting (C)	Weights (Ws)	Watering (Wg)
TC1	2	400 g	3 kg/h	Compacting	No Weights	No watering
TC2	6	400 g	3 kg/h	Compacting	Weights	No watering
TC3	2	400 g	4 kg/h	Compacting	No Weights	No watering
TC4	2	350 g	4 kg/h	Compacting	No Weights	No watering
TC5	3	400 g	4 kg/h	No Compacting	No Weights	No watering
TC6	1	400 g	3 kg/h	No Compacting	No Weights	No watering
TC7	1	400 g	3 kg/h	No Compacting	Weights	No watering
TC8	1	545 g	4 kg/h	No Compacting	No Weights	No watering
TC9	4	400 g	4 kg/h	No Compacting	No Weights	112 g of water
TC10	1	400 g	4 kg/h	No Compacting	No Weights	224 g of water

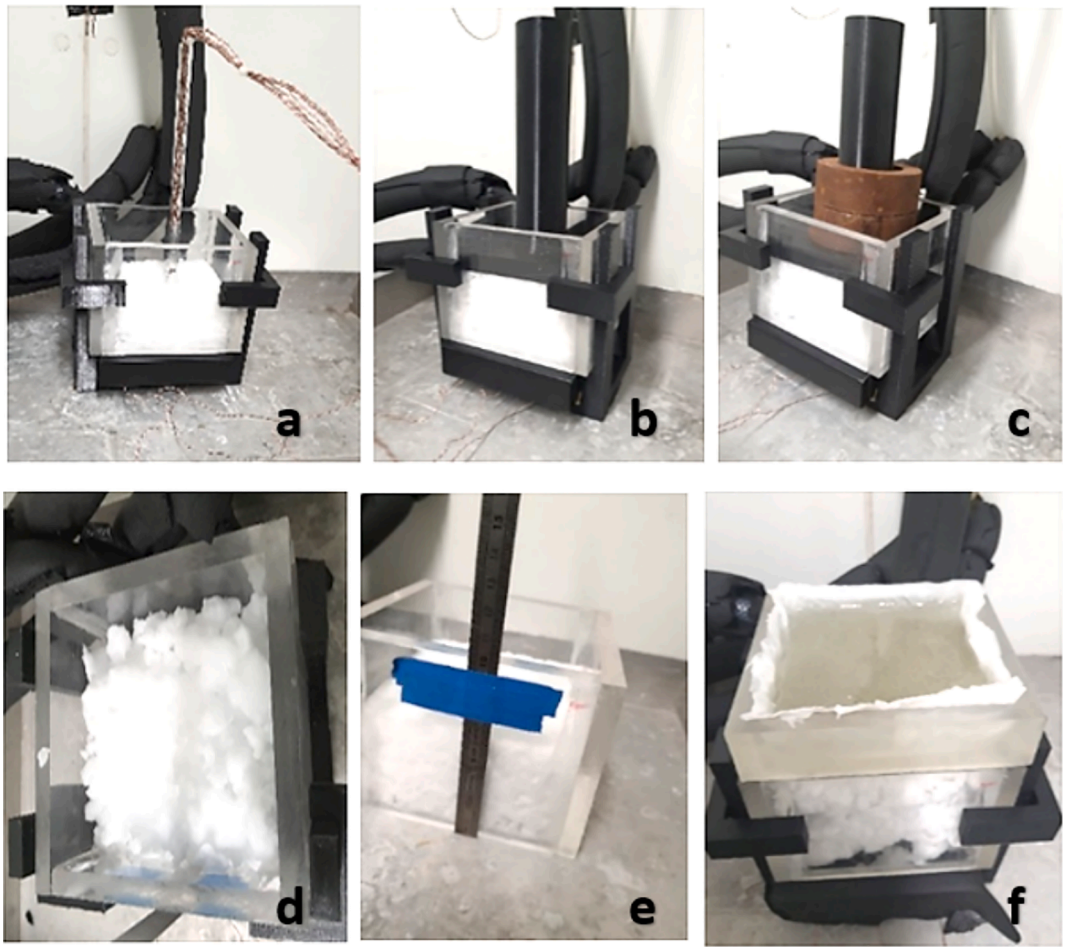

Fig. 6. Illustration of the different experiments carried out for ice melting process: C_NWs_NWg **(a, e)**; C_Ws_NWg **(b, c)**; NC_NWs_NWg **(d)**; NC_NWs_Wg **(f)**.

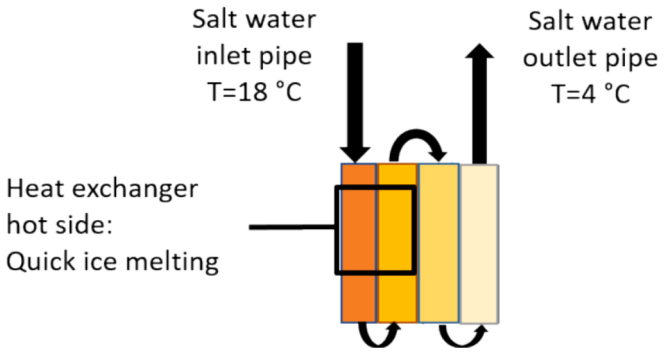

Fig. 7. Diagram of the circulation of salt water in the heat exchanger.

the salt water inlet pipe) melted faster than the other one (Fig. 7). The watering flow rate was calculated to be approximately 0.6 kg/h. The hand-held tamper and the weights weighed 0.13 kg and 1.62 kg, respectively. The salinity of the salt water solution and the freshwater obtained after melting was measured for each experiment.

2.4. Assessment of ice melting process

To evaluate the ice melting process, the melting efficiency (E) was calculated as a metric for the energy transfer efficiency between the ice and salt water. This calculation quantifies the actual energy absorbed by the salt water compared to the energy available in the ice (1).

$$E = \frac{\text{Energy absorbed}}{\text{Energy available}} = \frac{\dot{m}_{st\_wr}\, c_{p_{st\_wr}} \int \Delta T_{melt} dt}{m_{ice} L_{melt}} \quad (1)$$

In ideal conditions, the melting efficiency would be 100 %, meaning that the ice would transfer all its energy to the salt water upon contact with the heat exchanger. However, due to real (non-ideal) conditions and irreversibilities, the efficiency is always less than 1. Quantifying this efficiency is crucial for process improvement. To simplify calculations, the sensible part in the energy available in the ice was neglected, and the heat capacity of seawater was assumed constant. As the temperature of the cold room (T = 2 °C) is much lower than that of the input salt water (T = 18 °C), regardless of whether ice was present on the heat exchanger, heat transfer occurred between the salt water and the surrounding air. Therefore, according to thermodynamics principles, the total heat released by the salt water corresponds to the addition of heat absorbed by the ice and the air next to the heat exchanger. This means that the decrease in salt water temperature during the experiments is not exclusively due to the ice melting but also influenced by the air inside the cold room. However, only the heat exchange with the ice needs to be considered when calculating the melting efficiency (1). Therefore, temperature difference calculations should be based on a baseline temperature that represents the salt water temperature without the influence of the surrounding air ($T < T_{inlet}$). This baseline is determined by placing the 3D hand-held tamper with weights directly above the heat exchanger to minimise the exchange between the salt water and the air. This step is performed after the ice has completely melted. Fig. 8 illustrates an example of the evolution of salted water temperatures at the inlet and outlet of the heat exchanger during the experiment and the

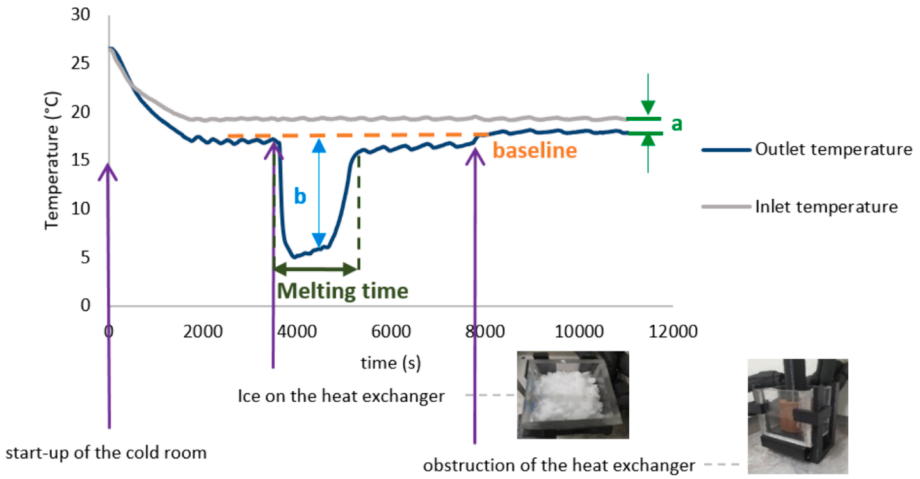

Fig. 8. Evolution of the salted water inlet and outlet temperatures vs time: **a)** ΔT air contribution; **b)** ΔT ice contribution.

determination of the baseline.

From Fig. 8, several data can be derived, including the minimum temperature reached by the salted water, the mean temperature difference between the inlet and outlet of the heat exchanger during melting, the melting time, the melting efficiency, the melting kinetic and the exchanged power. The melting time is the time between the sudden drop in the heat exchanger outlet temperature (corresponding to putting the ice on the heat exchanger) and the start of its stabilisation after a further rise, marking the end of the ice melting. To calculate the melting efficiency, $\int \Delta T_{melt} dt$, which represents the temperature difference during melting, was determined using the trapezoidal rule for calculating the area between the outlet temperature curve and the baseline. For the watering tests, the energy absorbed by the watering water was removed to obtain the real melting efficiency. The melting kinetic is given by dividing the quantity of ice used by the melting time (2). The melting kinetic by surface area can be approximated with the heat transfer area (3)). The exchanged power was determined by dividing the melting efficiency by the melting time (4). Analysis of the impact of the operating conditions on these parameters will allow the melting process to be optimised. The propagation of uncertainty was used to determine each objective function's uncertainty from the measurements' uncertainties. The law of propagation of uncertainty when measuring a quantity f, which depends on two variables x and y, with x and y being uncorrelated, is given by (5). Table 2 presents the combined uncertainty (k = 2).

$$\text{Melting kinetic } (\dot{m}_{melt}) = \frac{\text{Quantity of ice}}{\text{Melting time}} = \frac{m_{ice}}{t_{melt}} \quad (2)$$

$$\text{Melting kinetic per unit area } (D) = \frac{\text{Melting kinetic}}{\text{heat transfer area}} = \frac{\dot{m}_{melt}}{A} \quad (3)$$

$$\text{Exchanged power } (\dot{Q}) = \frac{\text{Melting efficiency}}{\text{Melting time}} = \frac{E}{t_{melt}} \quad (4)$$

$$\text{Propagation of uncertainty}(\sigma_f) = \sqrt{\left(\frac{\partial f}{\partial x}\right)^2 {\sigma_x}^2 + \left(\frac{\partial f}{\partial y}\right)^2 {\sigma_y}^2} \quad (5)$$

2.5. Preliminary study: Determination of the heat transfer area available for ice melting

A preliminary study was conducted to determine the heat transfer area experimentally, as there was no available data on the heat transfer area of the used heat exchanger. Characterising the heat transfer area of the heat exchanger is not crucial for the ice melting analysis. However, determining the melting kinetics per unit area is valuable for future scale-up considerations. It allows a more accurate determination of the surface area required to achieve a specific mass flow rate of freshwater production.

The heat transfer area (A) can be determined using the heat transfer equation for a heat exchanger (6).

$$\dot{Q}_{exchanged} = \dot{Q} = U \times A \times LMTD \qquad \Rightarrow A = \frac{\dot{Q}}{U \times LMTD} \quad (6)$$

From (6), there are two significant unknowns: the heat transfer area (A) and the overall heat transfer coefficient (U). To calculate A, the heat exchanger was subjected to natural convection in the cold room (T = 2 °C). Water flowed through the heat exchanger at 3 kg/h with an inlet temperature constant at 19 °C. Four thermocouples were used to determine the logarithmic mean temperature difference (LMTD). One thermocouple was placed at the inlet pipe of the heat exchanger and another at the outlet pipe to measure the temperature difference of water. The other two thermocouples were placed on the fins on both sides of the heat exchanger to measure the air temperature. The value of U was estimated at 12 W/(m^2.°C) [20], corresponding to natural convection. The experiment was repeated twice and each variable was calculated using (7) and (8). Table 3 shows the results found.

$$\dot{Q} = \dot{m}_{wr} \times c_{p_{wr}} \times \Delta T \quad (7)$$

Table 2
Propagation of uncertainty.

Calculated quantity	Maximum Uncertainty
Melting efficiency (E)	± 2 %
Melting kinetic ($\dot{m}_{melt}$)	± 0.002 kg/h
Melting kinetic per unit area (**D**)	± 0.06 kg/h.m^2
Exchanged power ($\dot{Q}$)	± 0.02 % of energy/min

Table 3
Heat exchanger heat transfer area determined experimentally.

	Test 1	Test 2	
$\dot{Q}$(W)	29.52	31.42	**Average heat transfer area (m^2)**
LMTD (°C)	8.0	7.8	
A(m^2)	0.309	0.335	**0.322 (±1.3 %)**

$$\mathrm{LMTD} = \frac{[(T_{i1} - T_{o2}) - (T_{o1} - T_{i2})]}{[\ln(T_{i1} - T_{o2}) - \ln(T_{o1} - T_{i2})]} \quad (8)$$

The average heat transfer area was found to be 0.322 m^2. In order to verify the result obtained and validate the method used, the heat transfer area was also determined geometrically by measuring the heat exchanger dimensions (9).

$$\text{Available heat transfer area} = \text{frontal surface } (\mathbf{A_{frontal}}) + \text{internal surface } (\mathbf{A_{internal}}) \quad (9)$$

The frontal surface is the surface in direct contact with the ice during melting (10). The internal surface is the surface in contact with the melted ice and the water (11).

$$\mathbf{A_{frontal}} = (N_{MPET} \times l_{HE} \times \varepsilon_{MPET} + N_{fin} \times l_{fin} \times \varepsilon_{fin}) \times 2 \quad (10)$$

$$\mathbf{A_{internal}} = A_{int\ MPET} + A_{int\ fin} \quad (11)$$

$$A_{int\ MPET} = N_{MPET} \times l_{HE} \times h_{HE} \times 2 - N_{fin} \times h_{HE} \times \varepsilon_{fin} \times 2 \quad (12)$$

$$A_{int\ fin} = N_{fin} \times h_{HE} \times l_{fin} \times 2 \quad (13)$$

N_{MPET} is the number of micro-multiport extrusion tubes where water circulates, and l_{MPET} and ε_{MPET} are the tube length and thickness, respectively. N_{fin} is the number of fins, and l_{fin} and ε_{fin} are the fin's length and thickness, respectively. l_{HE} and h_{HE} are the length and height of the heat exchanger exchanging part, respectively. Table 4 shows the results obtained for the available heat transfer area.

The internal surface area available is greater than the frontal surface. Indeed, it corresponds to more than 96 % of the total available heat transfer area. The heat transfer area found by measurements is realistic and in accordance with the one determined in the natural convection experiment with a standard deviation of ± 0.3 %. Therefore, during the natural convection experiment, almost all the available heat transfer area participated in the heat transfer; this will likely not be the case during ice melting experiments.

3. Results and discussion

Fig. 9 illustrates the evolution of salt water temperature at the heat exchanger outlet during the **TC5** test conditions. The three temperature curves exhibit identical patterns, indicating consistent melting times. This repeatability confirms the reliability of the ice melting test methodology. Table 5 presents a comparative analysis of the objective functions calculated for each repetition. These objective functions are salinity before and after desalination, melting time, melting kinetic per unit area, mean temperature difference between the inlet and outlet of the heat exchanger, minimum temperature reached at the heat exchanger outlet during melting, melting efficiency and exchanged power. The data found further affirms the consistency and reproducibility of the experiments.

The shape of the curves already shows an impact on the melting time due to the change in operating conditions, with consistency between repetitions. Table 6 gives the mean values of the objective functions calculated for each type of experiment. The standard deviations calculated for the tests with repetition are reasonable (Table 6). Analysing all this data makes it possible to define, study and compare the impact of operating conditions (optimisation parameters: ice quantity, salt water flow rate, ice compaction, etc.) on the objective functions (melting time, melting efficiency, etc.).

Table 4
Heat exchanger heat transfer area measured.

	MPET	Fins	Total
$\mathbf{A_{frontal}}$ (m^2)	0.0016	0.0043	0.0117
$\mathbf{A_{internal}}$ (m^2)	0.0247	0.2908	0.3156
Available heat transfer area (m^2)			**0.327**

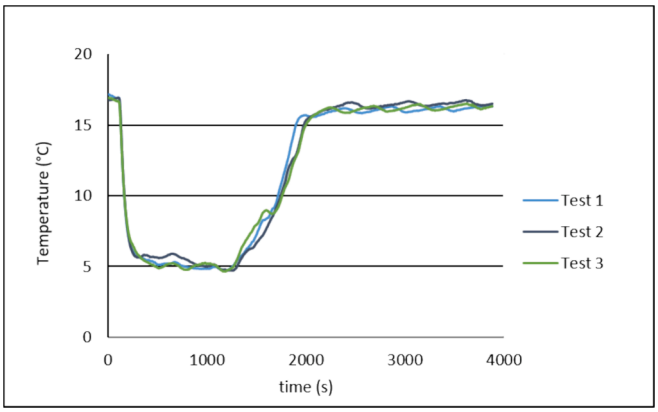

Fig. 9. Evolution of heat exchanger outlet temperature vs time for test conditions **TC5.**

3.1. Effect of ice quantity and salt water flow rate

Fig. 10 shows the effect of salt water flow rate and ice quantity on the melting efficiency of the heat exchanger when using compacted and non-compacted ice.

The effect of salt water flow rate can be studied by comparing test conditions **TC5** with **TC6** and **TC1** with **TC3** (Table 1; Table 6). Increasing the salt water flow rate by 33 % (TC5) compared with the initial flow rate of 3 kg/h (TC6) resulted in a 13 % increase in the minimum temperature at the heat exchanger outlet (T_{min}), a 3 % increase in the mean temperature difference (ΔT_{mean}), a 33 % increase in the melting efficiency (E), a 15 % decrease in melting time (t_{melt}) and a 57 % increase in the exchanged power ($\dot{Q}$): improvements in overall heat transfer performance. In the case of compacted ice, when the flow rate of salt water is increased by 33 % (TC3) compared with the initial flow rate of 3 kg/h (TC1), a better heat exchange was also obtained: 11 % increase in T_{min}, 28 % increase in ΔT_{mean}, 24 % increase in E, 28 % decrease in t_{melt} and 74 % increase in $\dot{Q}$. Increasing the salt water flow rate increases the melting efficiency and decreases the melting time due to a better heat transfer coefficient between the ice and the salt water. Compacting the ice before melting doesn't change the tendency. In a continuous system (overall process), it will not be possible to control the melting time by playing freely with the salt water flow rate due to its direct correlation with the required quantity of freshwater (quantity of ice). Nevertheless, it is reassuring to know that an increase in freshwater demand will not reduce the process's overall performance.

Test conditions **TC3**, **TC4**, **TC5** and **TC8** can be used to analyse the effects of ice quantity (Table 1; Table 6). Increasing the quantity of ice initially at 400 g (TC5) by 145 g (TC8) with a salt water flow rate of 4 kg/h, without compacting or adding weights or water on the top of the ice, led to a 6 % increase in T_{min}, a 3 % decrease in ΔT_{mean}, a 6 % decrease in E, a 24 % increase in t_{melt} and a 24 % decrease in $\dot{Q}$. The negative impact of increasing the quantity of ice on melting time is expected as it is a logical relationship: more latent energy is available in the ice for the same absorption capacity of the salt water. However, an increase in the ice quantity also triggers a more significant increase in the salt water flow rate aligned with the freshwater demand. This counteracts the effect on melting time. Reducing the amount of ice compacted initially at 400 g (TC3) by 50 g (TC4) with a salt water flow rate of 4 kg/h, without adding weight or water, had almost no effect on t_{melt} with a gain of 6 % in T_{min} and a loss of 4 % in ΔT_{mean}, and 2 % in E and $\dot{Q}$. For the tests with compacting, decreasing the ice quantity by 12.5 % does not seem to be sufficient to affect the melting time. Only the minimum temperature at the heat exchanger outlet and ΔT_{mean} are

Table 5
Comparison of objective functions obtained for test conditions **TC5.**

TC5	Salinity before/after (PSU)	Melting time t_{melt} (min)	Melting kinetic per unit area **D**(kg/h.m^2)	Mean temperature difference ΔT_{mean} (°C)	Minimum temperature T_{min} (°C)	Efficiency **E** (%)	Exchanged power $\dot{Q}$ (% of energy/min)
Test 1	30.25 /3.13	37.8	1.97	12.46	4.69	69.99	1.85
Test 2	30.94 /3.30	39	1.91	12.47	4.73	78.19	2.00
Test 3	30.04 /3.06	35.3	2.11	12.15	4.65	67.77	1.92
Average	30.41 /3.16	37.39	1.99	12.36	4.69	71.98	1.92

Table 6
Objective functions obtained for each type of experiment.

Test conditions	Salinity before/after (PSU)	t_{melt}(min)	Melting kinetic per unit area **D** (kg/h.m^2)	ΔT_{mean}(°C)	T_{min} (°C)	**E** (%)	$\dot{Q}$ (% of energy/min)
TC1 400 g; 3 kg/h C_NWs_NWg	30.51 /2.98	43.42 (±5.07)	1.70 (±0.20)	10.20 (±0.39)	4.32 (±0.15)	54.60 (±6.24)	1.26 (±0.00)
TC2 400 g; 3 kg/h C_Ws_NWg	29.98 /2.98	40.22 (±2.30)	1.83 (±0.11)	10.41 (±0.49)	3.59 (±0.20)	53.28 (±3.68)	1.33 (±0.12)
TC3 400 g; 4 kg/h C_NWs_NWg	30.08 /3.09	31.08 (±2.47)	2.37 (±0.19)	13.03 (±0.20)	4.81 (±0.11)	67.72 (±0.36)	2.19 (±0.19)
TC4 350 g; 4 kg/h C_NWs_NWg	30.36 /3.22	31.17 (±2.12)	2.07 (±0.14)	12.46 (±0.02)	5.08 (±0.16)	66.41 (±0.64)	2.14 (±0.17)
TC5 400 g; 4 kg/h NC_NWs_NWg	30.61 /3.16	37.39 (±1.87)	1.99 (±0.08)	12.36 (±0.18)	4.69 (±0.04)	71.98 (±5.49)	1.92 (±0.08)
TC6 400 g; 3 kg/h NC_NWs_NWg	30.25 /2.88	44.17	1.66	12.00	4.16	54.18	1.23
TC7 400 g; 3 kg/h NC_Ws_NWg	30.94 /3.06	44	1.67	11.46	4.45	62.56	1.42
TC8 545 g; 4 kg/h NC_NWs_NWg	30.82 /3.12	46.33	2.16	11.98	4.95	67.83	1.46
TC9 400 g; 4 kg/h NC_NWs_Wg (112 g)	30.50 /2.49	35.83 (±2.91)	2.06 (±0.16)	11.52 (±0.25)	4.87 (±0.23)	61.29 (±1.28)	1.72 (±0.14)
TC10 400 g; 4 kg/h NC_NWs_Wg (224 g)	30.23 /2.21	35.17	2.09	11.33	4.81	60.65	1.72

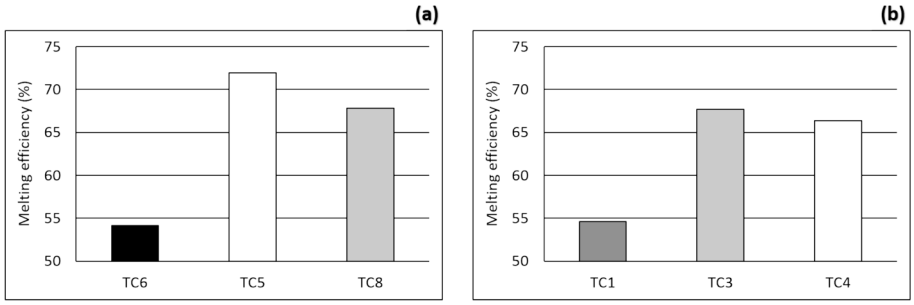

Fig. 10. Melting efficiency: impact of salt water flow rate and ice quantity without compacting **(a)** and with compacting **(b)**.

significantly impacted. In a continuous system, the reduction in ice quantity will be triggered by a decrease in the salt water flow rate (direct correlation). According to the results obtained, increasing or decreasing the ice quantity has the opposite effect of increasing or decreasing the salt water flow rate. Consequently, the flow rate of salt water and the quantity of ice will naturally compensate for each other impact on melting time and melting efficiency.

3.2. Effect of compacting and using weights

At the end of the separation stage, the ice collected is in the form of snow. Tests were carried out with compacted ice and non-compacted ice. Plus, weights were put on top of the ice during some experiments to ensure that the melting was uninterrupted. Fig. 11 and Fig. 12 show the impact of compacting the ice before the melting stage and using

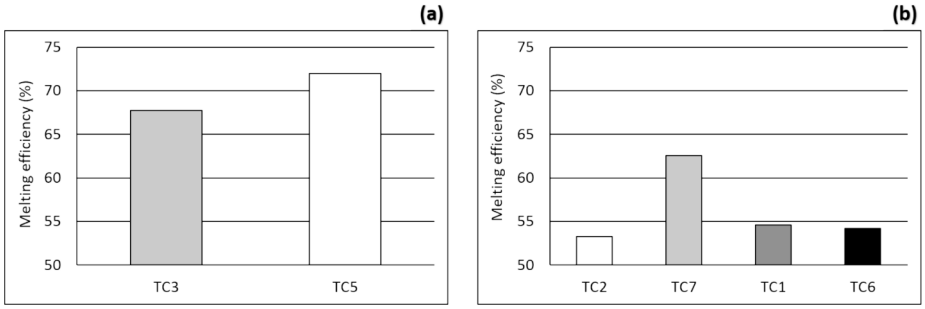

Fig. 11. Melting efficiency: impact of ice compaction and weights for a salt water flow rate of 4 kg/h **(a)** and 3 kg/h **(b)**.

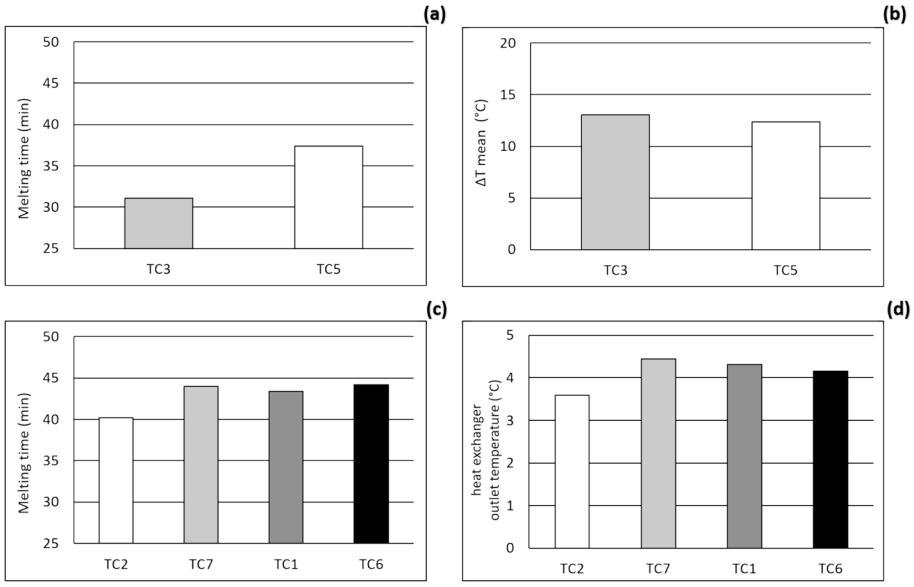

Fig. 12. Impact of ice compaction and weights on melting time, mean temperature difference and heat exchanger outlet temperature for a salt water flow rate of 4 kg/h **(a, b)** and 3 kg/h **(c, d)**.

weights during the melting stage.

The effect of ice compaction was observed in test conditions **TC1**, **TC3**, **TC5** and **TC6** (Table 1; Table 6). Compacting 400 g of ice before melting with a salt water flow rate of 4 kg/h, without using weights or adding water (TC3), compared with not compacting it under the same conditions (TC5), resulted in a 3 % increase in the minimum temperature at the heat exchanger outlet (T_{min}), a 5 % increase in the mean temperature difference (ΔT_{mean}), a 6 % decrease in the melting efficiency (E), a 17 % decrease in melting time (t_{melt}) and an increase of 13 % in the exchanged power ($\dot{Q}$). Compacting 400 g of ice with this time a salt water flow rate of 3 kg/h (TC1) compared to no compaction under the same conditions (TC6) resulted in + 4 % in T_{min}, − 15 % in ΔT_{mean}, + 1 % in E, − 2 % in t_{melt} and + 2 % in $\dot{Q}$. Compacting before melting allows better heat exchange inside the block of ice, which melts faster. The effect on the melting time is more pronounced when the salt water flow rate is 33 % higher. As the ice melts faster, the proportion of energy absorbed per time by the salt water ($\dot{Q}$) increases. A slight increase in E (energy absorbed by the salt water/energy available) is observed for the tests with a low salt water flow rate, and a decrease is observed for the tests with a high flow rate (Fig. 11). This is unexpected but can be explained by the fact that during the melting tests with a salt water flow rate of 4 kg/h, the average temperature measured in the cold room was slightly higher than during the tests with 3 kg/h, resulting in greater heat loss through the air. This may also explain the opposite behaviour observed for ΔT_{mean}. Although compacting is not essential for the process function correctly, it does offer advantages in terms of ΔT_{mean} and t_{melt} (Fig. 12).

The use of weights during the melting process was analysed for compacted **(TC1, TC2)** and non-compacted ice **(TC6, TC7)** (Table 1; Table 6). Using weights on top of 400 g of non-compacted ice generated + 7 % in T_{min}, − 4 % in ΔT_{mean}, + 15 % in E and $\dot{Q}$ and almost no effect on t_{melt}. Using weights, this time, on top of 400 g of compacted ice caused − 17 % in T_{min} , + 2 % in ΔT_{mean}, − 2 % in E, − 7 % in t_{melt} and + 6 % in $\dot{Q}$. The use of weights during melting tests has a different impact depending on whether the ice is compacted or not. The weights on top of the ice limit the heat transfer with the air in the cold room, which increases melting efficiency. The reduction in melting efficiency for tests with compacted ice could be due to greater heat loss through the walls of the acrylic column because of better heat transfer inside the ice block. The hardening of the ice after compaction may be the reason for the lower increase in power exchanged during tests with compacted ice. Like compacting, the use of weights is not necessary for the process. However, it is beneficial when aiming for very low temperatures at the heat exchanger outlet (Fig. 12). The lower the seawater temperature, the lower the energy required to produce the ice slurry. These two operating conditions can be employed for a given period when these performance outcomes are desired.

3.3. *Effect of watering*

Fig. 13 shows the impact of watering the ice during the melting stage. Test conditions **TC5**, **TC9** and **TC10** were used for the analysis.

Watering the ice during melting with 112 g of water for 400 g of ice, a salt water flow rate of 4 kg/h, without compacting or adding weights (TC9), caused a 4 % increase in the minimum temperature at the heat exchanger outlet (T_{min}), a 7 % decrease in the mean temperature difference (ΔT_{mean}), a 15 % decrease in the melting efficiency (E), a 4 % decrease in melting time (t_{melt}) and a 10 % decrease in the exchanged power ($\dot{Q}$). Doubling the amount of water (224 g) (TC10) caused + 3 % in T_{min}, − 8 % in ΔT_{mean}, − 16 % in E, − 6 % in t_{melt} and − 10 % in the $\dot{Q}$. In general, faster melting of the ice was observed as the ice exchanged heat with the salt water circulating underneath in the heat exchanger MPET and with the water droplets falling from the water tank. Watering, therefore, facilitated ice melting by slightly reducing the melting time. Doubling the water amount in the reservoir does not change the impact on the objective functions, as the watering flow rate does not change. The reduction in melting efficiency is entirely predictable since the watering water melts parts of the ice, reducing the amount of energy available for the salt water to absorb. An improvement in the homogeneity of the melting was also observed during both experiments. Indeed, the melting rate of the ice below the four drilled holes was similar to that of the ice on the hottest part of the heat exchanger, reducing the ΔT_{mean} between the heat exchanger inlet and outlet pipe. Although watering did not significantly enhance the process performance, it achieved the initial objective of obtaining a homogeneous melting throughout the heat exchanger.

Each investigated operating condition has a distinct impact on the ice melting process. It is essential to comprehend these conditions to effectively manage the melting process. Depending on the desired objective, certain operating parameters take precedence over others. For example, to improve melting efficiency, one thing to do is to increase the

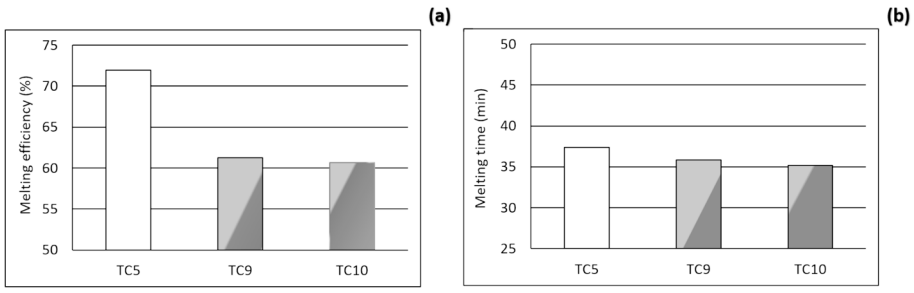

Fig. 13. Impact of watering on melting efficiency **(a)** and melting time **(b)**.

flow rate of salt water and use weights on non-compacted ice without watering. However, as these parameters are interrelated, optimising one aspect (e.g., melting efficiency) may have conflicting effects on another aspect (e.g., melting time). Therefore, trade-offs and concessions are inevitable.

4. Conclusion

An innovative desalination concept providing freshwater and cooling to an end-user has been evaluated based on lab-scale experiments. The ice melting stage, the focus of this study, was characterised using real desalination conditions in a batch system. The melting efficiency is directly influenced by the salt water flow rate and the quantity of ice. Increasing the salt water flow rate by 33 % for 400 g of ice without compacting, watering or using weights resulted in a 33 % improvement in melting efficiency. However, increasing the ice quantity by 36 % with a salt water flow rate of 4 kg/h led to a 6 % decrease in melting efficiency. Compacting the ice enhanced the mean temperature difference between the heat exchanger inlet and outlet and reduced the melting time. The use of weights to force contact between the ice and the heat exchanger during melting was helpful to reduce significantly the temperature at the outlet of the heat exchanger. Watering the ice during melting facilitated and homogenised the melting process. Given the results obtained, using the ice slurry desalination technique for the simultaneous supply of freshwater and cooling to a seaside hotel seems promising. In future work, the finned-tube heat exchanger will be modelled and optimised to increase the melting efficiency and the experimental set up will be studied in a continuous process. Moreover, the performances of the whole desalination/cogeneration project, integrating ice slurry production and all the heat exchangers, will also be analysed.

CRediT authorship contribution statement

Maria Aurely Yedmel: Writing – original draft, Methodology, Formal analysis, Investigation, Data Curation, Visualization. **Ahmad Nasser eddine:** Writing – review & editing. **Hong-Minh Hoang:** Writing – review & editing, Supervision. **Romuald Hunlede:** Conceptualization, Writing – review & editing, Supervision. **Laurence Fournaison:** Conceptualization, Writing – review & editing, Supervision. **Anthony Delahaye:** Conceptualization, Writing – review & editing, Supervision.

Declaration of competing interest

The authors declare that they have no known competing financial interests or personal relationships that could have appeared to influence the work reported in this paper.

Data availability

Data will be made available on request.

References

[1] Y. Ai, Y. Yan, G. Dong, S. Han, Investigation of microstructure evolution process in circular shaped oscillating laser welding of Inconel 718 superalloy, Int. J. Heat Mass Transf. 216 (2023) 124522.
[2] A.A. Al-Abidi, S. Mat, K. Sopian, M.Y. Sulaiman, A.T. Mohammad, Internal and external fin heat transfer enhancement technique for latent heat thermal energy storage in triplex tube heat exchangers, Appl. Therm. Eng. 53 (2013) 147–156.
[3] N.A. Amran, S. Samsuri, N. Safiei, Z.Y. Zakaria, M. Jusoh, Review: Parametric Study on the Performance of Progressive Cryoconcentration System, Chem. Eng. Commun. 203 (2015).
[4] Antonov, I., J., Locarnini, R. A., Boyer, T. P., Mishonov, A. V. & Garcia, H. E. 2006. World Ocean Atlas 2005, Volume 2: Salinity. S. Levitus. Ed. NOAA Atlas NESDIS 62 ed. U.S. Government Printing Office, Washington.
[5] D. Curto, V. Franzitta, A. Guercio, A Review of the Water Desalination Technologies, Appl. Sci. 11 (2021).
[6] M. Darwish, Desalination Process: A Technical Comparison, in: Proceedings of the IDA World Congress on Desalination and Water Sciences. s.l.:s.n.
[7] K. Fujii, M. Yamada, Enhancement of melting heat transfer of ice slurries by an injection flow in a rectangular cross sectional horizontal duct, Appl. Therm. Eng. 60 (2013) 72–78.
[8] J. Gasia, N.H.S. Tay, M. Belusko, L.F. Cabeza, F. Bruno, Experimental investigation of the effect of dynamic melting in a cylindrical shell-and-tube heat exchanger using water as PCM, Appl. Energy 185 (2017) 136–145.
[9] D. Groulx, M. Lacroix, Study of close contact melting of ice from a sliding heated flat plate, Int. J. Heat Mass Transf. 49 (2006) 4407–4416.
[10] B. Kalista, H. Shin, J. Cho, A. Jang, Current development and future prospect review of freeze desalination, Desalination 447 (2018) 167–181.
[11] A.D. Khawaji, I.K. Kutubkhanah, J.-M. Wie, Advances in seawater desalination technologies, Desalination 221 (2008) 47–69.
[12] W. Lin, M. Huang, A. Gu, A seawater freeze desalination prototype system utilizing LNG cold energy, Int. J. Hydrogen Energy 42 (2017) 18691–18698.
[13] Z. Liu, Z. Quan, Y. Zhao, H. Jing, L. Wang, X. Liu, Numerical research on the solidification heat transfer characteristics of ice thermal storage device based on a compact multichannel flat tube-closed rectangular fin heat exchanger, Energy 239 (2022) 122381.
[14] S. Mi, L. Cai, K. Ma, Z. Liu, Investigation on flow and heat transfer characteristics of ice slurry without additives in a plate heat exchanger, Int. J. Heat Mass Transf. 127 (2018) 11–20.
[15] H. Neumann, V. Palomba, A. Frazzica, D. Seiler, U. Wittstadt, S. Gschwander, G. Restuccia, A simplified approach for modelling latent heat storages: Application and validation on two different fin-and-tubes heat exchangers, Appl. Therm. Eng. 125 (2017) 41–52.
[16] B. Niezgoda-Żelasko, Heat transfer in the melting of ice slurry during flow in a vertical slit channel, Exp. Therm Fluid Sci. 153 (2024) 111133.
[17] J. Pássaro, A. Rebola, L. Coelho, J. Conde, G.A. Evangelakis, C. Prouskas, D. G. Papageorgiou, A. Zisopoulou, I.E. Lagaris, Effect of fins and nanoparticles in the discharge performance of PCM thermal storage system with a multi pass finned tube heat exchange, Appl. Therm. Eng. 212 (2022) 118569.
[18] Pronk, p., infante ferreira, c. a. & witkamp, g. j., Superheating of ice slurry in melting heat exchangers, Int. J. Refrig 31 (2008) 911–920.
[19] M.I. Rashad, H.A. Faiad, A.T. Ghonim, S. Ahmed, M.A. Farahat, Single-stage freezing desalination study with slurry pressing piston and enhanced vacuum for brine extraction, Desalination 566 (2023) 116947.
[20] E. Rouland, Les Échangeurs Thermiques- Les échangeurs à faisceaux complexes- Échangeurs frigorifiques, P.80 [Online]. Eric Rouland, AREELIS Technologie, Université de Rouen. Available: http://talbourdel.yves.free.fr/resources/DOC/cours-iup-me-echangeurthermique-2.pdf [Accessed 2022].
[21] J.S. Sangwai, R.S. Patel, P. Mekala, D. Mech, M. Busch, Desalination of seawater using gas hydrate technology—Current status and future direction. In Proceedings of the 18th International Conference on Hydraulics, Water Resources, Coastal and Environmental Engineering, HYDRO 2013 International, 2013 Madras, India. 434–440.
[22] H. Sharon, K.S. Reddy, A review of solar energy driven desalination technologies, Renew. Sustain. Energy Rev. 41 (2015) 1080–1118.
[23] S. Thongwik, T. Kiatsiriroat, A. Nuntaphan, Heat transfer model of slurry ice melting on external surface of helical coil, Int. Commun. Heat Mass Transfer 35 (2008) 1335–1339.

[24] H.S. Truong-Lam, S. Kim, S.D. Seo, C. Jeon, J.D. Lee, Water Purifying by Gas Hydrate: Potential Applications to Desalination and Wastewater Treatments, Chem. Eng. Trans. 78 (2020) 67–72.
[25] J. Wei, P. Chen, Y. Pan, Z. Fang, T. Fu, J. Zhang, G. Meng, J. Zhu, L. Zhang, Centrifugation forced ice-concentrate separation to enhance suspension freezing desalination performance, Desalination 566 (2023) 116919.
[26] M.A. Yedmel, R. Hunlede, S. Lacour, G. Alvarez, A. Delahaye, D. Leducq, A novel approach combining thermosiphon and phase change materials (PCM) for cold energy storage in cooling systems: A proof of concept, Int. J. Refrig 158 (2024) 393–404.